MODELIRANJE ČASOVNE VRSTE KOORDINAT GNSS IN NJIHOVE INTERAKCIJE S POVPREČNO MAGNITUDO POTRESOV

MODELLING OF THE TIME-SERIES OF GNSS COORDINATES AND THEIR INTERACTION WITH AVERAGE MAGNITUDE EARTHQUAKES

Sanja Tucikešić, Dragan Blagojević

SI | EN

IZVLEČEK

V prispevku predstavljamo analizo podatkov časovnih vrst koordinat postaj GNSS z uporabo spektralne analize po metodi najmanjših kvadratov (LSSA). Opravka smo imeli s časovnimi vrstami koordinat GNSS, v katerih so bile prisotne diskontinuitete. Ena od metod LSSA za zaznavanje in karakterizacijo periodičnih signalov v neenakomerno vzorčenih podatkih je metoda Lomb-Scargle. Analizirali smo podatke časovnih vrst postaje SRJV (Sarajevo) za približno dvajset let in postaje BEOG (Beograd) za približno pet let. Spektralna analiza se uporablja tudi za določitev prevladujočega šuma v časovni vrsti koordinat. Spektralni indeksi šuma (α) časovnih vrst koordinat GNSS postaj SRJV in BEOG so v območju −1≤α≤1 in opisujejo stacionarni stohastični proces. V nadaljevanju smo analizirali podatke časovnih vrst koordinat med petimi potresi v bližini postaj SRVJ in BEOG ter ocenili spektralne indekse šuma po odstranitvi linearnih, letnih in poletnih variacij v časovnih vrstah koordinat.

ABSTRACT

In this article the time series data of GNSS station coordinates are analysed, using least-squares spectral analysis (LSSA). One type of LSSA, the method of estimating a frequency spectrum, is the Lomb–Scargle method. Because of the presence of discontinuities in GNSS measurements, we applied Lomb–Scargle model for detecting and characterizing periodicity. We analyzed time series data from the station SRJV (Sarajevo), for a period of about 20 years, and BEOG (Belgrade), for a period of about 5 years. The spectral analysis is used to determine quickly the predominant noise in the position time series. Analyzed spectral indices of noise (α) of GNSS coordinate time series of SRJV and BEOG are in the range of −1≤α≤1, and describe stationary stochastic process. Then we processed time-series data of two GNSS station coordinates during 5 earthquakes that occurred near SRVJ and BEOG stations and estimated spectral indices of power-law noise from postfit residuals after removing linear, annual and semi-annual variation in the position time series.

KLJUČNE BESEDE

časovne vrste koordinat GNSS; spektralna analiza; model Lomb-Scargle; potres

KEY WORDS

time series of GNSS coordinates; spectral analysis; Lomb-Scargle model; earthquake

Sanja Tucikešić, Dragan Blagojević | MODELIRANJE ČASOVNE VRSTE KOORDINAT GNSS IN NJIHOVE INTERAKCIJE S POVPREČNO MAGNITUDO POTRESOV | MODELLING OF THE TIME-SERIES OF GNSS COORDINATES AND THEIR INTERACTION WITH AVERAGE MAGNITUDE EARTHQUAKES | 525-540 |

| 525 |

SI | EN

1 INTRODUCTION

Today, time series of GNSS coordinates are commonly used for the purpose of geophysical research and have proven to be useful in the research of the cycles of seismic deformations which relate to the whole seismic cycle (Feigl et al., 1990; Beutler et al., 1987; Foulger et al., 1987; Kellogg and Dixon, 1990). Co-seismic, post-seismic and inter-seismic crustal deformations can be reliably estimated using daily coordinates of time series from GNSS permanent stations. The established PGGA continual network (Permanent GPS Geodetic Array) in California (Bock et al., 1993) and the national network in Japan (Miyazaki et al., 1996) provided some of the first reliable results of seismic deformations based on high-precision GNSS measurements (Bock et al., 1993).

Crustal deformation analysis in seismogenically active areas is one of the most important applications of GNSS. The territories of Bosnia and Herzegovina and Serbia, our study region, are poorly studied in terms of their geodynamics, based on GNSS techniques allowing the estimation of the crustal deformation at different scales both in time and in space. Serbia and Bosnia and Herzegovina are located between the Carpathian-Balkans mountain system and the compressive geotectonic contact of the Dinarides and the Adriatic microplate. The Dinarides absorb the motion of the Adriatic microplate which causes present-day deformation. The seismicity of our study region occurs at the low level but it frequently suggests the continual tectonic activity of the Dinarides. Similar studies in other active regions are commonly based on the analysis of time-series from GNSS permanent stations.

For the purpose of this research, we used time-series data from the station SRJV (Sarajevo) for the period from June 1999 to March 2019, and the BEOG station (Belgrade), for the period from August 2014 to March 2019. Coseismic deformation is investigated using these stations. Daily GPS time series data from SRJV and BEOG stations in the IGS08 reference frame are available from the Nevada Geodetic Laboratory at http://geodesy.unr.edu/NGLStationPages/GlobalStationList/.

2 MATHEMATICAL MODEL OF TIME SERIES OF GNSS COORDINATES

Any arranged series of measurements, realized in different epochs, usually in identical time intervals, is called a time series. A time series allows monitoring of statistical changes of some physical phenomena. Models of time series have different forms and can represent different4stochastic processes. Time series are usually classified as models in the time or frequency domains. A model in the time domain is based on time series monitoring as a time function. On the other hand, a model in the frequency domain analyzes mathematical functions, or a signal, with regard to frequencies.

A time series consists of four components (Mann, 1995): trend component $T(t)$, cyclic component $C(t)$, seasonal component $S(t)$, with $E(t)$ representing a component of other random or systematic instabilities. A time-series aims at the statistical investigation of each of the mentioned four components and how effective the value is on the event. Interaction between these components helps to understand the time series. This interaction between them is classified as either additive or multiplicative. In a multiplicative time series, the components multiply together to make the time series (if the trend is increasing, the amplitude of seasonal activity is increasing). In an additive time series, the components

Sanja Tucikešić, Dragan Blagojević | MODELIRANJE ČASOVNE VRSTE KOORDINAT GNSS IN NJIHOVE INTERAKCIJE S POVPREČNO MAGNITUDO POTRESOV | MODELLING OF THE TIME-SERIES OF GNSS COORDINATES AND THEIR INTERACTION WITH AVERAGE MAGNITUDE EARTHQUAKES | 525-540 |

| 526 |

add together to make the time series (if the trend is increasing, the absolute value is growing, but changes stay relative). Therefore, a time series can be expressed in the following manner:

$$X(t) = T(t) \times C(t) \times S(t) \times E(t),$$ (1)

$$X(t) = T(t) + C(t) + S(t) + E(t)$$

where the argument t is the time of the series observation. Traditional methods of the time series analysis mainly work on the decomposition of the trend change, and on identifying seasonal and cyclic changes. Any other remaining signal can be attributed to other unidentified accidental or systematic instabilities. The spectral analysis used to determine the predominant noise in the time series of GNSS coordinates actually refers to the analysis of the $E(t)$ component (Li et al., 1999).

In geophysical research, the trend estimation of GNSS time series represents a starting point. Apart from significant episode deformations, such as major earthquakes, a linear trend may represent a good indicator of the way the site moves inter-seismically. In time series describing geophysical processes, noise is usually time-correlated, which can seriously affect the accuracy of the linear trend estimation, e.g. velocity and its standard deviation (Langbein, 2004). Linear changes can be explained through tectonic plates motions, whereas non-linear changes are mainly caused by unidentified internal errors related to the GNSS equipment, as well as by external geophysical effects such as coseismic earthquakes.

A mathematical model (2) that can be used in analyzing the coordinate components of GNSS daily time series is (see e.g. Dingcheng, 2017):

$$y(t_i) = a + \sum_{i=1}^{n} b_i(t_i - t_0)^i + \sum_{i=1}^{n_p} (c_i \sin(2\pi t_i / p_i) + d_i \cos(2\pi t_i / p_i)) +$$
$$+ \sum_{j=1}^{n_g} g_j H(t_i - t_{g_j}) + \sum_{i=1}^{n_A} (c_{A_i} + AH \ln(1 + \frac{t_i - t_{eq}}{\tau})) + \sum_{i=1}^{n_e} (t_{e_i})$$ (2)

where: y - daily solutions of a time series of GNSS coordinates , a - position of the station, b_i - linear velocity of the station, t - time, c_i and d_i - describes annual and semi-annual amplitudes of periodical motions (harmonic components are included into the model of annual, seasonal and higher frequency time-dependent phenomena), $n_p = 2$, $p_1 = 2$ year, $p_2 = 0.5$ year, $\sum_{j=1}^{n_g} g_j H(t_i - t_{g_j})$ - describes

sudden phenomena caused by equipment or seismic events for any given number of deviations n_g of the element g and epoch t_{g_j}, using the Heaviside function (unit step function applied in signal processing in order to present the signal that changes its condition) , t_{eq} - representing the time of earthquake (referring to the time of the main impact), c - co-seismic motion after the earthquake (represented by logarithmic or exponential function, data offset caused by post-seismic relaxation with a logarithmic or exponential decay), A - amplitude of simplified - Omori law, τ - denoting the time delay of post-seismic deformation after the main impact and t_{e_i} - denoting measurement errors, namely, all remaining changes that can be attributed to other accidental or systematic instabilities. By least-squares adjustment, the model parameters are estimated assuming different models for the coloured noise.

Sanja Tucikešić, Dragan Blagojević | MODELIRANJE ČASOVNE VRSTE KOORDINAT GNSS IN NJIHOVE INTERAKCIJE S POVPREČNO MAGNITUDO POTRESOV | MODELLING OF THE TIME-SERIES OF GNSS COORDINATES AND THEIR INTERACTION WITH AVERAGE MAGNITUDE EARTHQUAKES | 525-540 |

| 527 |

The most common stochastic models for t_{e_i} are those presented in Williams (2003) and Williams (2008). In those papers, t_{e_i} is assumed to have a power spectrum that depends on the frequency f according to the form given in Williams (2003):

$$P(f) = P_0 (f / f_0)^{\alpha},$$
(3)

where: f - spatial or time frequency, f_0 and P_0 - normalisation constants and α - spectral index. Based on the value of α, different stochastic processes can be described with this model. If α is in the range $-1 \leq \alpha \leq 1$, fractional Gaussian motion, t_{e_i} is a stationary stochastic process. For $|\alpha| > 1$, fractional Brownian motion, t_{e_i} is non-stationary (Mandelbrot 1977). They represent a solid indicator of the noise source characterisation. Special cases of spectral indexes are white noise ($\alpha = 0$), flicker noise ($\alpha = -1$) and random-walk noise of Brownian motion ($\alpha = -2$). Figure 1 illustrates the noise spectrum and the associated names given to the integer values.
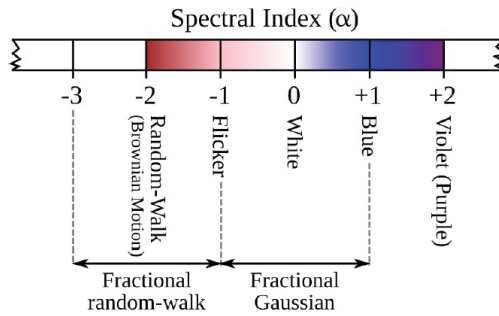

Figure 1: Spectral index of noise in geophysical phenomena (M. A. Goudarzi et al., 2015).

We estimated spectral indices from post-fit residuals after removing linear, annual, and semi-annual signals as well as probable jumps in the position time series using Eq. (2). Generally, it is possible to fit the power-law function given in Eq. (3) to a periodogram obtained by Fast Fourier Transformation (FFT) and estimate P_0 and α. The FFT is a traditional method for determining the power spectrum. It requires evenly distributed data. It cannot be used in data containing gaps, which is a common case with a time-series of GNSS coordinates. Using interpolation methods several artefacts are then introduced to the data in both time and frequency domains, especially when the gap is large (Press et al.,1992). Therefore, in this study, we use the Lomb-Scargle algorithm to calculate the periodogram of post-fit residuals per station per position direction (Lomb 1976; Scargle 1982). This method has the advantage of evaluating the data of a time series of GNSS coordinates only at measured epochs, gives periodic signals in unevenly distributed observations, and evaluates logarithmic Lomb-Scargle power spectrum of a time-series of GNSS coordinates. The normalized Lomb-Scargle periodogram (normalized spectral power as a function of frequency) P_x of a time series of GNSS coordinates $y(t_i)$ for $i = 1, 2, ..., N$ is estimated by Mao et al. (1999):

$$P_x(\omega) = \frac{1}{2\sigma^2} \left\{ \frac{\left[\sum_{j=1}^{N} \left(y_j - \overline{y} \right) \cos \omega (t_j - \tau) \right]^2}{\sum_{j=1}^{N} \cos^2 \omega (t_j - \tau)} + \frac{\left[\sum_{j=1}^{N} \left(y_j - \overline{y} \right) \sin \omega (t_j - \tau) \right]^2}{\sum_{j=1}^{N} \sin^2 \omega (t_j - \tau)} \right\},$$
(4)

Sanja Tucikešić, Dragan Blagojević | MODELIRANJE ČASOVNE VRSTE KOORDINAT GNSS IN NJIHOVE INTERAKCIJE S POVPREČNO MAGNITUDO POTRESOV | MODELLING OF THE TIME-SERIES OF GNSS COORDINATES AND THEIR INTERACTION WITH AVERAGE MAGNITUDE EARTHQUAKES | 525-540 |

| 528 |

where: ω - angular frequency ($\omega = 2\omega f > 0$), σ - root mean square (RMS) $\sigma = \sqrt{\dfrac{1}{N-1}\sum\limits_{j=1}^{N}(x_j - \bar{x})^2}$ and

$\bar{x}$ - means value $\bar{x} = \dfrac{1}{N}\sum\limits_{j=1}^{N}x_j$, the constant τ is defined as an offset - $\tan(2\omega\tau) = \sum\limits_{j=1}^{N}\sin 2\omega t_j \ / \sum\limits_{j=1}^{N}s\cos 2\omega t_j$.

The periodogram is calculated in the range of the Nyquist frequency. The power of noise is plotted in dB using logarithm function to base 10 as:

$$P_x(f) = 10 \cdot \log_{10}\left(\frac{P_v}{fs}\right), \tag{5}$$

where: P_v is the power spectrum of the post-fit residuals estimated from Eq. (4) and f_s is the sampling frequency with the unit of day^{-1}. Then, the spectral index α of the power-law process (3) is estimated as the slope of the spectra in log-log space using Nikolaidis (2002):

$$\alpha = \frac{P_x(f)}{10 \cdot \log_{10}(f)}. \tag{6}$$

To process a time series we used TSAnalyzer, GNSS Time Series Analysis Software developed at the Geodesy and Dynamics Laboratory at the Institute of Geodesy and Geophysics in China (Dingcheng et al., 2017). Software package TSAnalyzer was written in Python and was developed for preprocessing and analyzing continuous GNSS position time series individually. It also provides a Lomb-Scargle spectrum analysis. Since it is based on Python, it is cross-platform software.

2.1 Methods for co-seismic and inter-seismic parameterization

The analysis of crustal deformations plays an important role in studies related to the whole seismic cycle. The seismic cycle stages can be estimated reliably using the time series of GNSS coordinates. Many seismogenic areas are monitored in this way (Hudnut, 2002). The seismic cycle refers to the notion of observing an earthquake before, during, and after its occurrence. In terms of crustal deformation, it can be divided into four-time phases: interseismic phase, preseismic phase, coseismic phase and postseismic phase (Figure 2).
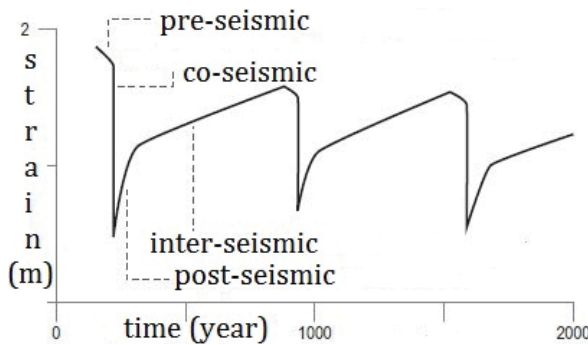

Figure 2:   Seismic cycles.

Interseismic slip, which accounts for most of the cycle, refers to the time between earthquakes. One of the significant inference from the measurement of fault zones by satellite surveying techniques is that

Sanja Tucikešić, Dragan Blagojević | MODELIRANJE ČASOVNE VRSTE KOORDINAT GNSS IN NJIHOVE INTERAKCIJE S POVPREČNO MAGNITUDO POTRESOV | MODELLING OF THE TIME-SERIES OF GNSS COORDINATES AND THEIR INTERACTION WITH AVERAGE MAGNITUDE EARTHQUAKES | 525-540 |

| 529 |

almost all major faults showed some stresses during the interseismic period (Wright et al., 2013). The pre-seismic phase refers to the time just before the earthquake arrives. Small magnitude earthquakes occur during this phase and some anomalies that represent the occurrence of a stronger earthquake may occur. The coseismic phase refers to the time of the earthquake when faults burst and seismic waves are generated. Earthquakes generate dynamic and static movements. Both of these movements cause changes in the Earth's crust and Earth's sheath that lead to other forms of deformation. Dynamically they are expanding, but after the seismic waves pass they return to their original positions, while static movements are permanent. Seismometers can record dynamic but not static movements, which requires additional surveying and instrumentation. Considering high-precision GNSS measurements, coseismic shifts make a significant contribution to understanding the dynamics of the Earth's surface. Earthquakes induce coseismic deformations in the crust and can create large changes in the position of geodetic stations, which are especially visible in the time series of GNSS positions.

The fourth phase of the seismic cycle is the postseismic phase that takes place after the earthquake and corresponds to the period of a few minutes to several years after the earthquake. It is reflected in the subsequent earthquakes (aftershocks) that follow the main stroke. This phase is the phase following movements that occur after an earthquake and the return of faults to the interseismic phase state.

In our study (Sarajevo, Koran, Valjevo and Turija), for all earthquakes JavaScript Object Notation (JSON) text format was used for processing. JSON offset file is created based on the data downloaded from USGS (U.S. Geological Survey) at https://earthquake.usgs.gov/earthquakes/search/ for earthquakes with magnitudes of 4 near SRVJ and BEOG stations for the time periods researched in this paper. Earthquakes recorded near the station SRVJ were downloaded from Earthquake Catalog near the location of Sarajevo at 43,792 N 18,452 E, 5,0 km depth, on 2009-03-31, and with M 4,1, and near the location of Koran at 43,761 N 18,569 E, 3,6 km depth, on 2015-04-12, with M 4,1; and near the station BEOG at the locations near Valjevo at 44,126 N 19,936 E, 9,0 km depth, on 2015-03-08, and with M 4,4, and Turija at 44,463 N 21,624 E, 2,0 km depth, on 2016-06-09, and with M 4,2. After that (JSON) text format is reloaded into TSAnalyzer software for further analysis. In this paper we analyzed real co-seismic deformations. Our strategy consists of processing data from our time series on the day of the earthquake. A significant number of studies use daily position time series to estimate the coseismic offsets, whereas the strategy used for the calculations varies. For instance, processing the data time series 4 days before the earthquake and 4 days after the earthquake to compute the coseismic offsets of 2013 Craig, Alaska, earthquake (Mw7.5), (Ding et al., 2015).

3 RESULTS OF NUMERICAL RESEARCH

3.1 Time series of GNSS coordinates of the station SRVJ

Our study was first performed for the time series of GNSS coordinate daily solutions of the station SRVJ for the period from June 1999 to April 2019 with the number of epochs equal to 4389 and the gap of 39.4%. To start the analysis, we first detrended the daily observation and solved semi-annual and annual signals. We estimated site velocity in the IGS08 frame. Semi-annual and annual signals per component were modelled using Eq. (2). The results are presented in Figure 3 and Table 1 (below).

Sanja Tucikešić, Dragan Blagojević | MODELIRANJE ČASOVNE VRSTE KOORDINAT GNSS IN NJIHOVE INTERAKCIJE S POVPREČNO MAGNITUDO POTRESOV | MODELLING OF THE TIME-SERIES OF GNSS COORDINATES AND THEIR INTERACTION WITH AVERAGE MAGNITUDE EARTHQUAKES | 525-540 |
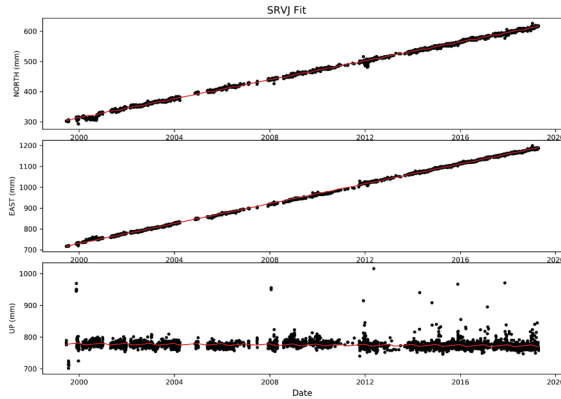
| 530 |

Figure 3: Detrending daily observations of the site SRVJ, including determining semi-annual and annual signals.

The estimated trend from the time series shows positive values for the horizontal component and negative values for the vertical component. The trend tends to increase in the direction of northeast (28.50 mm/year). Estimated horizontal components have smaller deviations than the vertical part. The Weighted Root Mean Square (WRMS) error estimation of the function for one year for coordinates and deformations is 3.16 mm for the horizontal component and 13.67 mm for the height component. A large WRMS value (up to 25.0 mm) for the height component can result from too large geophysical anomalies, which affect changes in GNSS station coordinates and cause inaccuracies in deformation modelling (Kaczmarek et al., 2018). This study shows that there are seasonal and semi-annual signals in all three coordinate components. It can be seen that the periodic components are different for the analyzed station SRVJ. However, the annual period is dominant. Annual variation is with typical amplitudes about 1 mm for horizontal and 2 mm for vertical.

Table 1: The results detrending daily observation of SRVJ including WRMS (Weighted Root Mean Squared), semi-annual and annual variation and estimated velocity in the IGS08 frame.

	SRVJ		
Solution	North component	**East component**	**Up component**
	WRMS: 2.99 mm	WRMS: 3.33 mm	WRMS: 13.67 mm
Station Velocities (IGS08):	15.67 ± 0.01 mm/yr	23.8 ± 0.01 mm/yr	−0.31 ± 0.03 mm/yr
Semi-annual variation (sin):	−0.73 ± 0.07 mm	−0.23 ± 0.07 mm	−0.08 ± 0.30 mm
Semi-annual variation (cos):	0.22 ± 0.06 mm	−0.01 ± 0.07 mm	0.80 ± 0.29 mm
Annual variation (sin)	1.11 ± 0.07 mm	0.19 ± 0.07 mm	−1.59 ± 0.30 mm
Annual variation (cos)	0.34 ± 0.06 mm	0.94 ± 0.07 mm	1.62 ± 0.29 mm

3.2 Spectral domain analysis of the SRVJ station

Next, spectral indices were estimated from post-fit residuals after removing linear, annual and semi-annual signals using Eq. (4) for three position directions of the station SRVJ. Figure 4 presents a stochastic character of a power-law spectral index of the examined station SRVJ. In general, spectral indices estimated for stations vary between −1.01 and −0.26, meaning we deal with different spectral characters of residuals. Power spectra of the station SRVJ was estimated for about 20 years of data. Spectral indices

Sanja Tucikešić, Dragan Blagojević | MODELIRANJE ČASOVNE VRSTE KOORDINAT GNSS IN NJIHOVE INTERAKCIJE S POVPREČNO MAGNITUDO POTRESOV | MODELLING OF THE TIME-SERIES OF GNSS COORDINATES AND THEIR INTERACTION WITH AVERAGE MAGNITUDE EARTHQUAKES | 525-540 |

| 531 |

were estimated as –1.01 ± 0.02, –0.78 ± 0.02 and –0.26 ± 0.02 for the east, north and up directions, respectively. Power spectrum analysis confirms that GPS time series also do not contain significant power at annual harmonic frequencies (with spectral indices $-1 < \alpha < 1$), which indicates the presence of repeating signals without significant impacts. However, unless accounted, those annual signals can affect the estimation of site velocities intended for high accuracy purposes such as plate tectonics and reference frames (Blewitt et al., 2002).

Analyzed spectral indices of the GNSS coordinate time-series of SRJV in the range of $-1 \leq \alpha \leq 1$, describe the stationary stochastic process. The estimated spectral index of the station SRVJ East component is $\alpha = -1$ and equals to flicker noise. A proper description of the noise characteristics is essential for the estimation of realistic velocity uncertainties and for the proper interpretations of geophysical phenomena. Stationarity means that the statistical properties of the process generating the time series do not change over time. It does not mean that the series does not change over time, only that the way it changes does not change itself over time. Stationary processes are a sub-class of a wider family of possible models of reality. This sub-class is much easier to model and investigate.
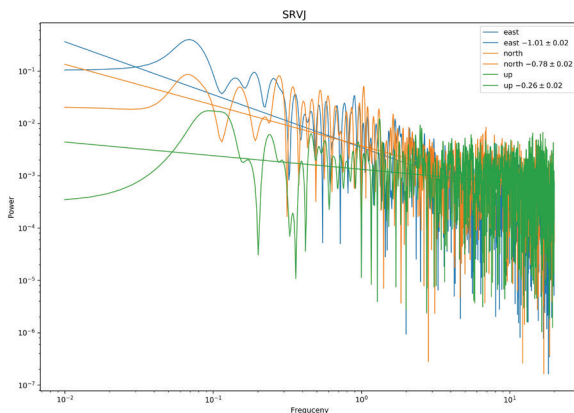

Figure 4: Spectral domain analysis obtained using Lomb-Scargle method, and the estimated spectral indices of the station SRVJ.

The final reason for stationarity is the importance of its ubiquity in the time series analysis of GNSS coordinates, making it possible to understand, detect and model as necessary for the application of many prominent tools and procedures in the time series analysis.

3.3 The use of GNSS coordinate time series of the station SRVJ to study 2009 and 2015 earthquakes near Sarajevo and Koran

Earthquakes from 2009 and 2015 near Sarajevo and Koran were next analyzed using data from the SRJV time series. Using Eq (2), it was determined how the earthquakes influenced station velocities on a particular day and at the particular time when the earthquake occurred (Figure 5a and Figure 5b). Table 2 and Table 3 show the estimated co-seismic velocities induced by earthquake.

Sanja Tucikešić, Dragan Blagojević | MODELIRANJE ČASOVNE VRSTE KOORDINAT GNSS IN NJIHOVE INTERAKCIJE S POVPREČNO MAGNITUDO POTRESOV | MODELLING OF THE TIME-SERIES OF GNSS COORDINATES AND THEIR INTERACTION WITH AVERAGE MAGNITUDE EARTHQUAKES | 525-540 |
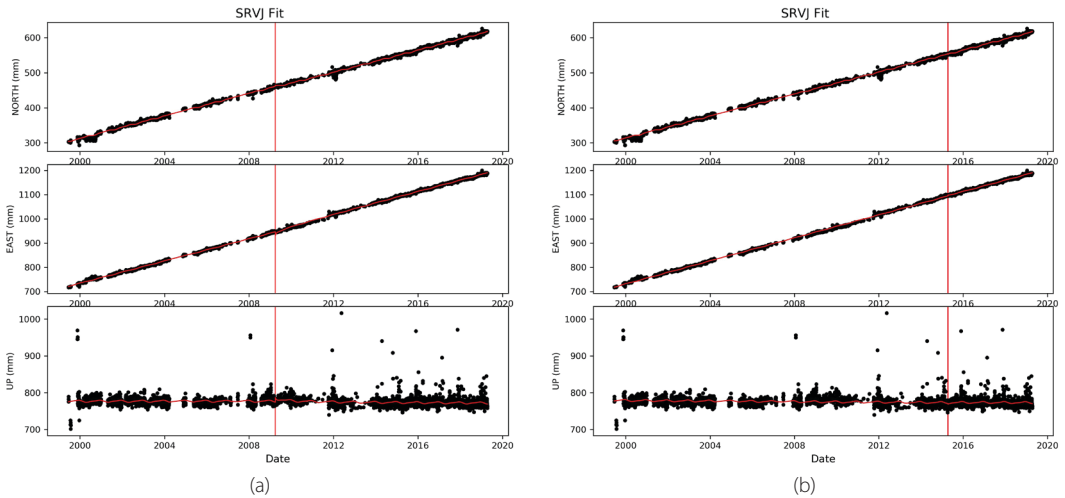
| 532 |

Figure 5: Model in the time domain, detrending daily observation of SRVJ including a semi-annual and annual variation with 2009 and 2015 earthquakes near Sarajevo (a) and Koran (b).

Table 2: The results detrending daily observation of SRVJ including semi-annual and annual variation and estimated velocity seismic event at the location Sarajevo 43,792 N 18,452 E, 5,0 km depth, 2009-03-31, M 4,1.

Solution	North component	East component	Up component
SRVJ with 2009 earthquake near Sarajevo			
	WRMS: 2.89 mm	WRMS: 2.62 mm	WRMS: 13.62 mm
Station Velocities (IGS08):	16.08 ± 0.02 mm/yr	22.90 ± 0.01 mm/yr	–0.31 ± 0.03 mm/yr
Semi-annual variation (sin):	–0.80 ± 0.06 mm	–0.23 ± 0.07 mm	–0.08 ± 0.30 mm
Semi-annual variation (cos):	0.24 ± 0.06 mm	–0.01 ± 0.07 mm	0.80 ± 0.29 mm
Annual variation (sin)	1.07 ± 0.06 mm	0.19 ± 0.07 mm	–1.59 ± 0.30 mm
Annual variation (cos)	0.26 ± 0.06 mm	0.94 ± 0.07 mm	1.62 ± 0.29 mm
Co-seismic velocities	3.59 ± 0.50 mm	–18.28 ± 0.45 mm	14.22 ± 2.42 mm

Table 3: The results detrending daily observation of SRVJ including semi-annual and annual variation and estimated velocity seismic event at the location Koran on 43,761 N 18,569 E, 3,6 km depth, 2015-04-12, M 4,1.

Solution	North component	East component	Up component
SRVJ with 2015 earthquake near Koran			
	WRMS: 2.99 mm	WRMS: 3.28 mm	WRMS: 13.67 mm
Station Velocities (IGS08):	15.68 ± 0.01 mm/yr	23.73 ± 0.01 mm/yr	–0.37 ± 0.05 mm/yr
Semi-annual variation (sin):	–0.76 ± 0.06 mm	–0.19 ± 0.07 mm	–0.12 ± 0.30 mm
Semi-annual variation (cos):	0.22 ± 0.06 mm	–0.01 ± 0.07 mm	0.81 ± 0.29 mm
Annual variation (sin)	1.13 ± 0.06 mm	0.22 ± 0.07 mm	–1.52 ± 0.30 mm
Annual variation (cos)	0.31 ± 0.06 mm	1.07 ± 0.07 mm	1.62 ± 0.30 mm
Co-seismic velocities	–1.72 ± 0.49 mm	4.93 ±- 0.54 mm	–1.94 ± 2.18 mm

Earthquakes induce coseismic deformations and can create changes in the position of geodetic stations, which are especially visible in the time series of GNSS coordinates. Earthquakes with magnitudes more than 8 significantly affect the position of GPS stations thousands of miles

Sanja Tucikešić, Dragan Blagojević | MODELIRANJE ČASOVNE VRSTE KOORDINAT GNSS IN NJIHOVE INTERAKCIJE S POVPREČNO MAGNITUDO POTRESOV | MODELLING OF THE TIME-SERIES OF GNSS COORDINATES AND THEIR INTERACTION WITH AVERAGE MAGNITUDE EARTHQUAKES | 525-540 |

| 533 |

away from the epicenter of the earthquake, taking into account the precision of GPS measurement today, which is at the level of several millimeters (Tregoning et al., 2013). Intermediate earthquake (magnitudes 6 to 8) can also have a significant impact on GPS station displacements (Metivier et al., 2014). Coseismic deformations obtained by processing the available earthquakes of magnitude ~ 4 do not show any significant changes with respect to the interseismic phase of the time series. Also, the spectral indices correspond to the stationary Gaussian process, (Figure 5a and Figure 5b).
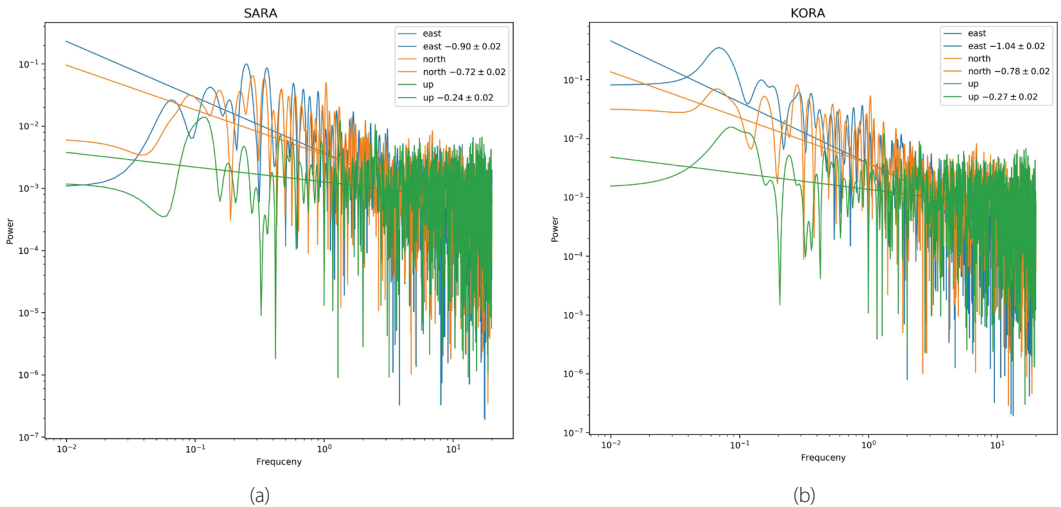

Figure 6:   Spectral domain analysis, method Lomb-Scargle and the estimated spectral indices of the station SRVJ for 2009 and 2015 earthquakes in Sarajevo (a) and Koran (b).

3.4 Time series of GNSS coordinates of the station BEOG

Our study was next performed for the time series of GNSS coordinate daily solutions of the station BEOG for the period from August 2014 to April 2019 with the number of epochs equal to 1615 and with the gap of 5.8%. To start the analysis we detrended the daily observations and determined the semi-annual and annual signals. We estimated site velocity in the IGS08 frame, and semi-annual and annual signals per component were modelled using Eq. (2). The results are presented in Figure 7 and Table 4 (below).

The estimated trend from the time series shows positive values for the horizontal component and negative values for the vertical component. The trend tends to increase in the direction of northeast (27.71 mm/year). Estimated horizontal components have smaller deviations than the vertical part. The Weighted Root Mean Square (WRMS) error estimation of a function for one year for coordinates and deformations is 2.31 mm for the horizontal component and 5.36 mm for the height component. This study shows that there are seasonal and semi-annual signals in all three coordinate components. It can be seen that the periodic components are different for the analyzed BEOG station. Also, the annual period is dominant. Annual variation is with typical amplitudes about 1 mm for horizontal and over 2 mm for vertical.

Sanja Tucikešić, Dragan Blagojević | MODELIRANJE ČASOVNE VRSTE KOORDINAT GNSS IN NJIHOVE INTERAKCIJE S POVPREČNO MAGNITUDO POTRESOV | MODELLING OF THE TIME-SERIES OF
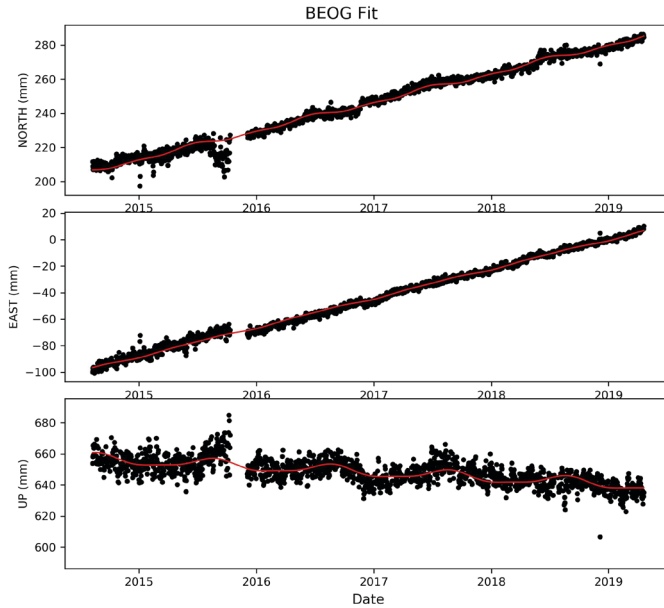GNSS COORDINATES AND THEIR INTERACTION WITH AVERAGE MAGNITUDE EARTHQUAKES | 525-540 |

| 534 |

Figure 7: Detrending daily observation of the site BEOG, including determining semi-annual and annual signals.

Table 4: The results detrending daily observation of BEOG including WRMS (Weighted Root Mean Squared), semi-annual and annual variation and estimated velocity in the IGS08 frame.

	BEOG		
Solution	North component	East component	Up component
	WRMS: 2.49 mm	WRMS: 2.13 mm	WRMS: 5.36 mm
Station Velocities (IGS08):	16.77 ± 0.05 mm/yr	22.06 ± 0.04 mm/yr	–3.69 ± 0.10 mm/yr
Semi-annual variation (sin):	–0.28 ± 0.09 mm	–0.01 ± 0.07 mm	0.80 ± 0.19 mm
Semi-annual variation (cos)	0.70 ± 0.09 mm	–0.33 ± 0.07 mm	–0.38 ± 0.19 mm
Annual variation (sin)	0.35 ± 0.09 mm	–0.15 ± 0.07 mm	–2.15 ± 0.19 mm
Annual variation (cos)	–0.93 ± 0.09 mm	–0.62 ± 0.08 mm	–2.20 ± 0.19 mm

3.5 Spectral domain analysis of the BEOG station

Next, spectral indices were estimated from post-fit residuals after removing linear, annual, and semi-annual signals using Eq. (4) for three position directions of the station BEOG. Figure 8 presents a stochastic character of a power-law spectral index of the examined station BEOG. In general, spectral indices estimated for stations vary between –0.88 and –0.38. Power spectra of the station BEOG was estimated for about 5 years of data.

Spectral indices were estimated as –0.88 ± 0.02, –0.74 ± 0.02 and –0.38 ± 0.02 for the east, north and up directions, respectively. Power spectrum analysis confirms that GPS time series also do not contain significant power at annual harmonic frequencies (with spectral indices $–1 < \alpha < 1$), which indicates the presence of repeating signals without significant impacts. Analyzed spectral indices of GNSS coordinate time-series of BEOG also describe the stationary stochastic process.
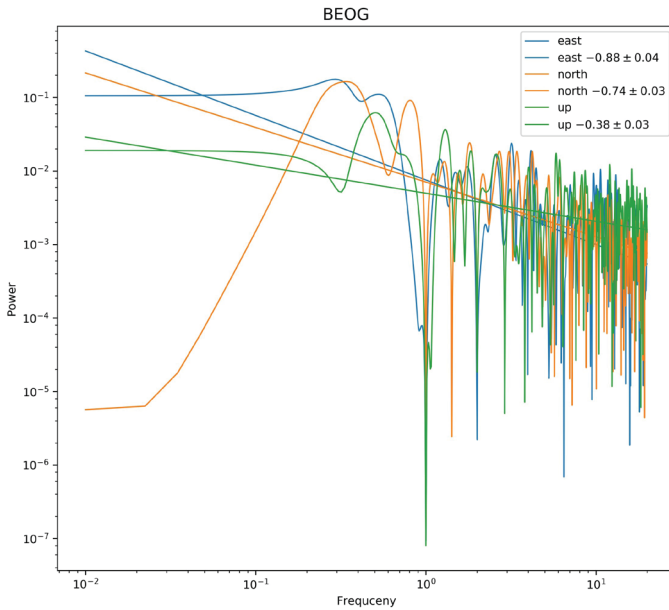
Sanja Tucikešić, Dragan Blagojević | MODELIRANJE ČASOVNE VRSTE KOORDINAT GNSS IN NJIHOVE INTERAKCIJE S POVPREČNO MAGNITUDO POTRESOV | MODELLING OF THE TIME-SERIES OF GNSS COORDINATES AND THEIR INTERACTION WITH AVERAGE MAGNITUDE EARTHQUAKES | 525-540 |

| 535 |

Figure 8: Spectral domain analysis using the Lomb-Scargle method and the estimated spectral indices of the station BEOG.

3.6 The use of GNSS coordinate time series of the station BEOG to study 2015 and 2016 earthquakes near Valjevo and Turija

Earthquakes from 2015 and 2016 near Valjevo and Turija were next analyzed using the GNSS time series at the site BEOG. Using Eq (2), we determined how the earthquakes influenced the station coordinates on the particular day and at the particular time when these earthquakes occured (Figure 9a and Figure 9b). Table 5 and Table 6 show the estimated motions induced by these two earthquakes.
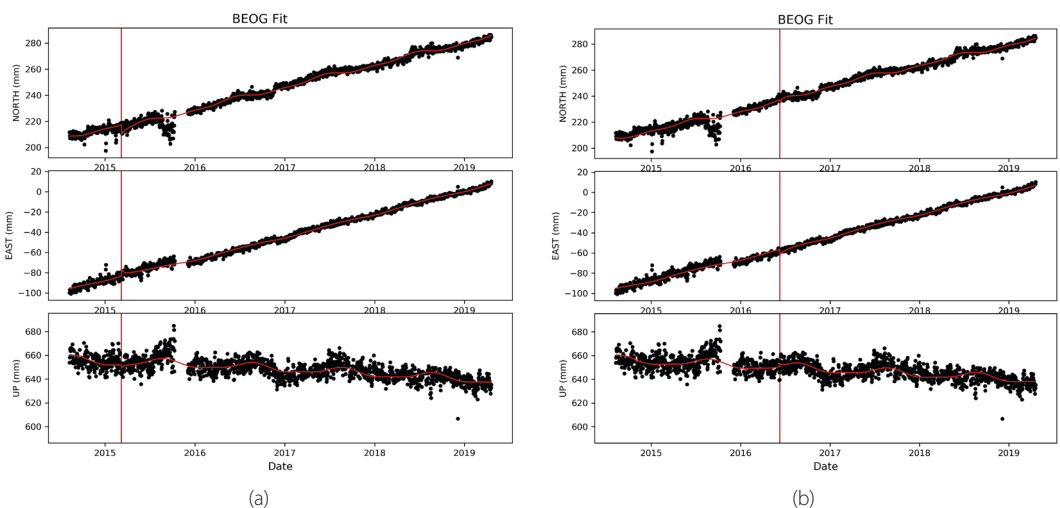

Figure 9: Model in the time domain of detrended daily observation at the site BEOG, including semi-annual and annual signals, for 2015 and 2016 earthquakes that occurred near Valjevo (a) and Turija (b).

Sanja Tucikešić, Dragan Blagojević | MODELIRANJE ČASOVNE VRSTE KOORDINAT GNSS IN NJIHOVE INTERAKCIJE S POVPREČNO MAGNITUDO POTRESOV | MODELLING OF THE TIME-SERIES OF GNSS COORDINATES AND THEIR INTERACTION WITH AVERAGE MAGNITUDE EARTHQUAKES | 525-540 |

| 536 |

Table 5:   The results detrending daily observation of BEOG including semi-annual and annual variations and estimated velocity seismic event at the location Valjevo 44,126 N 19,936 E, 9,0 km depth, 2015-03-08, M 4,4.

Solution	North component	East component	Up component
	BEOG with seismic event at the locality of Valjevo		
	WRMS: 2.34 mm	WRMS: 1.91 mm	WRMS: 5.34 mm
Station Velocities (IGS08):	16.53 ± 0.11 mm/yr	23.72 ± 0.09 mm/yr	−4.62 ± 0.26 mm/yr
Semi-annual variation (sin):	−0.35 ± 0.08 mm	−0.01 ± 0.07 mm	0.82 ± 0.19 mm
Semi-annual variation (cos):	0.67 ± 0.08 mm	−0.15 ± 0.07 mm	0.48 ± 0.19 mm
Annual variation (sin)	0.70 ± 0.09 mm	−0.31 ± 0.07 mm	2.12 ± 0.19 mm
Annual variation (cos)	−1.28 ± 0.09 mm	−0.80 ± 0.07 mm	2.03 ± 0.20 mm
Co-seismic velocities	−7.84 ± 0.71 mm	8.18 ± 0.59 mm	3.38 ± 1.68 mm

Table 6:   The results detrending daily observation of BEOG including semi-annual and annual variations and estimated velocity seismic event at the location Turija on 44,463 N 21,624 E, 2,0 km depth, 2016-06-09, M 4,2.

| Solution	North component	East component	Up component
	BEOG with a seismic event at the locality of Turija		
	WRMS: 2.34 mm	WRMS: 1.99 mm	WRMS: 5.36 mm
Station Velocities (IGS08):	14.96 ± 0.13 mm/yr	21.06 ± 0.11mm/yr	−3.41 ± 0.30 mm/yr
Semi-annual variation (sin):	−0.30 ± 0.08 mm	0.02 ± 0.07 mm	0.80 ± 0.19 mm
Semi-annual variation (cos):	0.77 ± 0.08 mm	−0.15 ± 0.07 mm	−0.43 ± 0.19 mm
Annual variation (sin)	0.73 ± 0.09 mm	−0.13 ± 0.07 mm	−2.16 ± 0.20 mm
Annual variation (cos)	−1.02 ± 0.09 mm	−0.90 ± 0.07 mm	−2.11 ± 0.20 mm
Co-seismic velocities	−2.63 ± 0.55 mm	−7.05 ± 0.46 mm	2.02 ± 1.24 mm
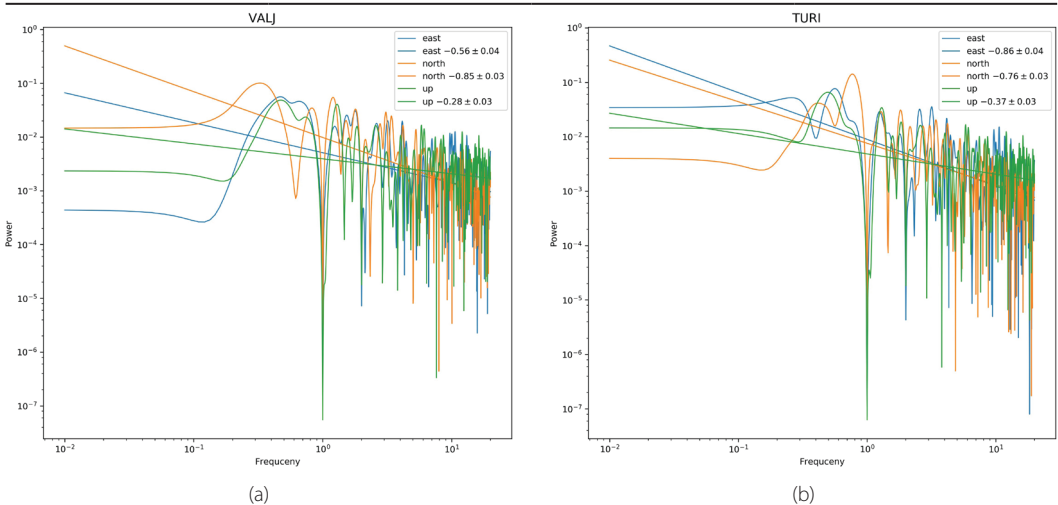
Figure 10: Spectral domain analysis using the Lomb-Scargle method and the estimated spectral indices of the station BEOG during 2015 and 2016 earthquakes near Valjevo (a) and Turija (b).

Postseismic deformations are usually in the same direction as the coseismic deformations. In general, postseismic deformations remain far smaller than coseismic deformation. However, postseismic accumulated deformations achieve a value usually as large as the coseismic deformations after 3–4 years of

Sanja Tucikešić, Dragan Blagojević | MODELIRANJE ČASOVNE VRSTE KOORDINAT GNSS IN NJIHOVE INTERAKCIJE S POVPREČNO MAGNITUDO POTRESOV | MODELLING OF THE TIME-SERIES OF GNSS COORDINATES AND THEIR INTERACTION WITH AVERAGE MAGNITUDE EARTHQUAKES | 525-540 |

| 537 |

deformations, (Trubienko et al., 2013). The coseismic deformations of the BEOG station obtained by processing the magnitudes 4.4 and 4.2 of the available earthquakes do not show any significant changes with respect to the interseismic phase of the time series. Also, the spectral indices correspond to the stationary Gaussian process, (Figure 10a and Figure 10b).

4 CONCLUSION

Spectral analysis time series of GNSS coordinates provides a key tool to quantify and understand tectonic movements. We used daily coordinate solutions of the stations SRVJ and BEOG, and performed analysis of those GNSS time series to obtain models of the series that fit best inter-seismic and co-seismic motions, taking into account trends and seasonal variations. The type of noise that flavours these data were obtained using a white spectral domain analysis, the Lomb-Scargle method, and post-fit residuals after removing linear, annual, and semi-annual signals. The Lomb-Scargle method was used for the power spectrum analysis because it does not require evenly distributed data. The time series of GNSS coordinates frequently contain missing data because of malfunction of GNSS receivers, power failure, removal of abnormal results, etc. The time series of GNSS coordinates have a gap of 39.4 % for the station SRVJ and the gap of 5.8 %. for the station BEOG.

The clean inter-seismic velocities we obtained here were calculated using described models Eq. (2), also calculated by means of the least-squares estimation with seasonal model, taking into account the annual and semi-annual periodicities. For the SRVJ station our estimated clean inter-seismic velocity is 15.67 ± 0.01 mm/yr, 23.8 ± 0.01 mm/yr, –0.31 ± 0.03 mm/yr in the north, east and up, respectively. For the BEOG station our estimated clean inter-seismic velocity is 16.77 ± 0.05 mm/yr, 22.06 ± 0.04 mm/ yr, –3.69 ± 0.10 mm/yr in the north, east and up, respectively. For both stations, variations are almost perfectly linear for the horizontal components that are east and north, and this clearly shows the tectonic motion. As a result of the trend analyses of time series, it was determined that stations were moving in the northeast direction 28.50 mm/year and 27.71 mm/year, for SRVJ and BEOG, respectively. This finding is consistent with the region's tectonic plate movements.

The vertical component includes significant seasonal variations. For the SRVJ station, our estimated annual periodicities are –1.59 ± 0.30 mm, 1.62 ± 0.29 mm of cycle sin and cycle cos, respectively. For the BEOG station our estimated annual periodicities are –2.15 ± 0.19 mm, –2.20 ± 0.19 mm of cycle sin and cycle cos, respectively. The coordinate time series of vertical components contain repeating annual cycles stemming from hydrological and atmospheric loading (Blewitt, et al., 2002). Without taking into account seasonal signals, it results in an increase in the auto-correlated or temporally correlated noise within a time series, which influences the stochastic model (Klos et al., 2018).

Knowledge of the spectral index is fundamental because it allows identification of the type of noise present in the time series. The values of spectral indices determined for SRVJ and BEOG have a range that corresponds to the fractional Gaussian noise, which is stationary, uncorrelated with time, and has statistical properties that are invariant over time. The spectral indices for the east component of the site SRVJ also require a flicker noise component. However, the origin of this flicker noise is still unclear. Flicker noise may simply be intrinsic to the GNSS system, due to errors in the GNSS observations or in their modelling (Rebischung et al., 2017). Several authors have suggested that white noise and flicker

Sanja Tucikešić, Dragan Blagojević | MODELIRANJE ČASOVNE VRSTE KOORDINAT GNSS IN NJIHOVE INTERAKCIJE S POVPREČNO MAGNITUDO POTRESOV | MODELLING OF THE TIME-SERIES OF GNSS COORDINATES AND THEIR INTERACTION WITH AVERAGE MAGNITUDE EARTHQUAKES | 525-540 |

| 538 |

noise, and to a smaller extent random walk, dominate GPS coordinate time series noise spectrum (Mao et al., 1999, Williams et al., 2004, Zhang et al., 1997).

When processing available earthquakes of magnitude ~ 4, the obtained coseismic velocities do not show any significant changes in the time series of GNSS coordinates, and they are in the range from -1.72 to -18.28 mm. Also, the estimated spectral indices for the SRVJ and BEOG stations during four earthquakes near Sarajevo, Koran, Valjevo and Turija are in the range of fractional Gaussian motion described. At the BEOG station, some fluctuations in the interseismic phase can be observed (between Valjevo and Turi earthquakes). This phenomenon was also observed at the SRVJ station between Sarajevo and Koran earthquakes, but of smaller magnitude. In this study, we see that each earthquake generates coseismic deformations in the region surrounding its epicentre. However, earthquakes with an average magnitude of about 4 do not cause significant discontinuities in the time series of GNSS coordinates. Bosnia and Herzegovina, and Serbia have a history of earthquakes of magnitude ~ 4 related to the tectonic activity in the Dinarides. Our analysis of time series coordinates, conducted using described models for four specific earthquakes, has given estimated coseismic station velocities. In order to better understand these events and their geodynamics, it is fundamental to the study of cinematics. Perfect modelling of cosmic deformations would be extremely complex as it would strongly depend on the local topographic and geological characteristics of the region. These results indicate that stations SRVJ and BEOG located in Bosna and Hercegovina and Serbia, respectively are rather stable and reliable and this described technique may be useful to others studying bigger or nearer earthquakes.

Literature and references:

Beutler, G., Bauersima, I., Gurtner, W., Rothacher, M., Schildknecht, T. (1987). Evaluation of the Alaska Global Positioning System Campaign with the Bernese Software. Journal of Geophysical Research: Solid Earth, 92 (B2), 1295−1303. DOI: https://doi.org/10.1029/jb092ib02p01295

Blewitt, D., Lavallee, D. (2002). Effect of annual signals on geodetic velocity. Journal of Geophysical Research: Solid Earth, 107 (7). DOI: https://doi.org/10.1029/2001jb000570

Bock, Y., Agnew, D., C., Fang, P., Genrich, J., F., Hager, B., H. (1993). Detection of crustal deformation from the Landers earthquake sequence using continuous geodetic measurements. Nature, 361 (6410), 337−340. DOI: https://doi.org/10.1038/361337a0

Ding, K., Freymueller, J. T., Wang, Q., Zou, R. (2015). Coseismic and early postseismic deformation of the 5 January 2013 Mw7.5 Craig earthquake from static and kinematic GPS solutions. Bulletin of the Seismological Society of America, 105 (2B), 1153−1164. DOI: https://doi.org/10.1785/0120140172

Dingcheng, W., Haoming, Y., Yingchun, S. (2017). TSAnalyzer, a GNSS time series analysis software. GPS Solutions, 21 (3), 1389−1394. DOI: https://doi.org/10.1007/s10291-017-0637-2

Feigl, K., L., Agnew, D., C., Bock, Y., Dong, D., Donnellan, A., Hager, B., H., Herring, T., A., Jackson, D., D., Jordan, T., H., King, R., W., Larsen, S., Larson, K., M., Murray, M., H., Shen, Z., Webb, F., H. (1993). Space geodetic measurement of crustal deformation in central and southern California. Journal of Geophysical Research: Solid Earth, 98 (B12), 677−712. DOI: https://doi.org/10.1029/93jb02405

Foulger, G. R., Bilham, R., Morgan, W., J., Einarsson, P. (1987). The Iceland GPS geodetic field campaign 1986. Eos, Transactions American Geophysical Union, 68(52), 1809−1813. DOI: https://doi.org/10.1029/eo068i052p01809-02

Hudnut, K. W. (2002). Continuous GPS observations of postseismic deformation following the 16 October 1999 Hector Mine, California, earthquake (Mw 7.1). Bulletin of the Seismological Society of America, 92 (4), 1403−1422. DOI: https://doi.org/10.1785/0120000912

Kaczmarek, A., Kontny, B. (2018). Estimates of seasonal signals in GNSS time series and environmental loading models with iterative least-squares estimation (iLSE) approach. Acta Geodynamica et Geomaterialia, 15 (2), 131−141. DOI: https://doi.org/10.13168/agg.2018.0009

Kellogg, J., N., Dixon, T., H. (1990). Central and South America GPS geodesy- CASA UNO. Geophysical Research Letters, 17 (3), 195−198. DOI: https://doi.org/10.1029/gl017i003p00195

Klos, A., Bos, M. S., Bogusz, J. (2018). Detecting time-varying seasonal signal in GPS position time series with different noise levels. GPS Solutions. 22 (1). DOI: https://doi.org/10.1007/s10291-017-0686-6

Langbein, J. (2004). Noise in two-color electronic distance meter measurements revisited. Journal of Geophysical Research: Solid Earth, 109 (B4). DOI: https://doi.org/10.1029/2003jb002819

Li, J., Miyashita, K., Kato, T., Miyazaki, S. (2000). GPS time series modeling by autoregressive moving average method: Application to the crustal deformation in central Japan. Earth Planets Space, 52 (3), 155−162. DOI: https://doi.org/10.1186/bf03351624

Sanja Tucikešić, Dragan Blagojević | MODELIRANJE ČASOVNE VRSTE KOORDINAT GNSS IN NJIHOVE INTERAKCIJE S POVPREČNO MAGNITUDO POTRESOV | MODELLING OF THE TIME-SERIES OF GNSS COORDINATES AND THEIR INTERACTION WITH AVERAGE MAGNITUDE EARTHQUAKES | 525-540 |

| 539 |

Lomb, N. R. (1976). Least-Squares Frequency Analysis of Unequally Spaced Data. Astrophysics and Space Science, 39 (2), 447–462. DOI: https://doi.org/10.1007/bf00648343

Mann, S. P. (1995). Statistics For Business and Economics. Wiley.

Mandelbrot, B. B. (1977). Fractals: form, chance and dimension. San Francisco, CA: Freeman.

Mao, A., Harrison, C. G. A., Dixon, T. H. (1999). Noise in GPS coordinate time series. Journal of Geophysical Research: Solid Earth, 104 (B2), 2797–2816. DOI: https://doi.org/10.1029/1998JB900033

Metivier, L., Collilieux, X., Lercier, D., Altamimi, Z., Beauducel, F. (2014). Global coseismic deformations, GNSS time series analysis, and earthquake scaling laws. Journal of Geophysical Research: Solid Earth, 119 (12), 9095–9109. DOI: https://doi.org/10.1002/2014jb011280

Miyazaki, S., Tsuji, H., Hatanaka, Y., Abe, Y., Yoshimura, A., Kamada, K., Kobayashi, K., Morishita, H., Iimura, Y. (1996). Establishment of the nationwide GPS array (GRAPES) and its initial results on the crustal deformation of Japan. Bulletin of GSI (Jpn.), 42, 27–41.

Moreira, R. J. S. (2013). Análise das características de ruído em series temporais GPS. PhD thesis. Lisboa, Portugal: Universidade de Lisboa.

Nikolaidis, R. (2002). Observation of geodetic and seismic deformation with the global positioning system. PhD thesis. SanDiego: University of California.

Press, W. H., Teukolsky, S. A., Vetterling, W. T., Flannery, B. P. (1992). Numerical Recipes in C: The Art of Scientific Computing. 2nd edition. New York, USA: Cambridge University Press.

Rebischung, P., Chanard, K., Metivier, L., Altamimi, Z. (2017). Flicker Noise in GNSS Station Position Time Series. American Geophysical Union, Fall Meeting 2017, abstract #G13A-04.

Scargle, J. D. (1982). Studies in astronomical time series analysis. II— statistical aspects of spectral analysis of unevenly spaced data. The Astrophysical Journal, 263, 835–853. DOI: https://doi.org/10.1086/160554

Tregoning, P., Burgette, R., McClusky, S. C., Lejeune, S., Watson, C. S., McQueen, H. (2013). A decade of horizontal deformation from great earthquakes. Journal of Geophysical Research: Solid Earth, 118 (5), 2371–2381. DOI: https://doi.org/10.1002/jgrb.50154

Trubienko, O., Fleitout, L., Garaud, J.-D., Vigny, C. (2013). Interpretation of interseismic deformations and the seismic cycle associated with large subduction earthquakes. Tectonophysics, 589, 126–141. DOI: https://doi.org/10.1016/j.tecto.2012.12.027

Williams, S. D. P. (2008). CATS: GPS coordinate time series analysis software. GPS Solutions, 12 (2), 147–153. DOI: https://doi.org/10.1007/s10291-007-0086-4

Williams, S. D. P., (2003). The effect of coloured noise on the uncertainties of rates estimated from geodetic time series. Journal of Geodesy, 76 (9–10), 483–494. DOI: https://doi.org/10.1007/s00190-002-0283-4

Williams, S. D. P., Bock, Y., Fang, P., Jamason, P., Nikolaidis, R. M., Prawirodirdjo, L., Miller, M., Johnson, D.J. (2004). Error analysis of continuous GPS position time series. Journal of Geophysical Research, 109, (B03). DOI: https://doi.org/10.1029/2003jb002741

Wright, T. J., Elliott, J. R., Wang, H., Ryder, I. (2013). Earthquake cycle deformation and the Moho: Implications for the rheology of continental lithosphere. Tectonophysics, 609, 504–523. DOI: https://doi.org/10.1016/j.tecto.2013.07.029

Zhang, J., Bock, Y., Johnson, H., Fang, P., Williams, S. D. P., Genrich, J., Wdowinski, S., Behr, J. (1997). Southern California Permanent GPS Geodetic Array: Error analysis of daily position estimates and site velocities. Journal of Geophysical Research: Solid Earth, 102 (B8), 18035–18055. DOI: https://doi.org/10.1029/97jb01380

Senior Teaching Assistant, Sanja S. Tucikešić
University of Banja Luka
Faculty of Architecture, Civil Engineering and Geodesy
Stepe Stepanovića 77 /3, 78000 Banja Luka,
Bosnia and Herzegovina,
e-mail: sanja.tucikesic@aggf.unibl.org

Prof. Dr. Dragan M. Blagojević
University of Belgrade Faculty of Civil Engineering
Bulevar kralja Aleksandra 73, 11000 Beograd,
Serbia
e-mail: bdragan@grf.bg.ac.rs

Sanja Tucikešić, Dragan Blagojević | MODELIRANJE ČASOVNE VRSTE KOORDINAT GNSS IN NJIHOVE INTERAKCIJE S POVPREČNO MAGNITUDO POTRESOV | MODELLING OF THE TIME-SERIES OF GNSS COORDINATES AND THEIR INTERACTION WITH AVERAGE MAGNITUDE EARTHQUAKES | 525-540 |

| 540 |

RECENZIRANI ČLANKI | PEER-REVIEWED ARTICLES

SI | EN